

# An Alignment and Integration Technique for Mirror Segment Pairs on the Constellation X Telescope

Theo Hadjimichael<sup>a</sup>, Scott Owens<sup>b</sup>, John Lehan<sup>c</sup>, Larry Olsen<sup>a</sup>, Timo Saha<sup>b</sup>, Tom Wallace<sup>b</sup>, Will Zhang<sup>b</sup>

<sup>a</sup>Ball Aerospace, 1616 McCormick Drive, Upper Marlboro, MD 20774

<sup>b</sup>NASA Goddard Space Flight Center, Greenbelt, Maryland 20771

<sup>c</sup>Center for Research and Exploration in Space Science and Technology, NASA Goddard Space Flight Center, and Department of Physics, University of Maryland, Baltimore County, 1000 Hilltop Circle, Baltimore, Maryland 21250

## Abstract

We present the concepts behind the current alignment and integration technique for a Constellation-X primary-secondary mirror segment pair prior to an x-ray beam line test. We examine the effects of a passive mount on thin glass x-ray mirror segments, and the issues of mount shape and environment on alignment. We also investigate how bonding and transfer to a permanent housing affects the quality of the final image.

## Passive spring-based mount Mattress intro

The mirror mounts currently being used in the “fabricate and assemble” testbed composed of two parts: a slumped glass cone, a.k.a., the cradle, and a set of 10 rows of mylar springs, a.k.a, the mattress. The springs are in fact long helical coils made of ~2 mm wide strips of aluminized mylar with a ~2 mm diameter glass rod bonded to each coil to provide a “spine” for each row of springs. Adjacent rows of springs alternate clockwise and counterclockwise directions to balance non-radial forces. There are 14 points of contact for the mirror per row. Each ~55 deg mirror weights ~ 42 g, measuring deflection of multiple coils around the edges of the mirror to be on average 6mm we calculated a spring constant  $k \approx -0.4$  N/m.

Two sets of primary/secondary mounts are employed, corresponding to either edge bonding or end bonding. Figure 1 shows the mount used for end bonding, the three screws will become the static points for mirror bonding and have like pairs on the opposite ends of the mount. Likewise, in Figure 2 there are five possible points of contact for edge bonding with corresponding points on the opposite edge. The mirrors for edge bonding are slightly larger, ~ 55° azimuthal span as opposed to the ~50° employed for end bonding.

The end bonding mounts were a first iteration mounting scheme and have a slight difference with respect to the edge bonding mounts in how the springs are utilized. While the main purpose of the mattress is to exert as little force per point of contact as possible, we can also perturb the cradle shape by raising and lowering each coil set slightly. While monitoring the full aperture focused image we can adjust the piston and tilt of each row of springs in order to minimize the impact of mount imperfections on the mirror shape. Thus, we are able to restore the shape of the mirror and create a better focus than is obtained immediately after placing a mirror segment on the mattress. The assumption is that we are countering environmental forces and allowing the mirror to assume its true shape, i.e., the shape the mirror wants to be after having been removed from the slumping mandrel.

For the end bonding mounts the springs were attached to a square kapton sheet, which was carefully centered onto the cradle. The mattress was then attached to the cradle at either edge only, allowing glass shims to be slid between the mattress and cradle to accomplish the shape restoration as determined by the focused image.

For the edge bonding mounts, the procedure is more sophisticated. The springs are now attached to free standing steel bars which are laid into aluminum channels attached to either end of the cradle. These channels have height adjustment screws which provide the piston/tilt adjustment capability that shims accomplished in the previous cradle design. These

mounts are only a temporary vehicle for co-alignment prior to moving to the permanent mount that becomes part of the final telescope structure.

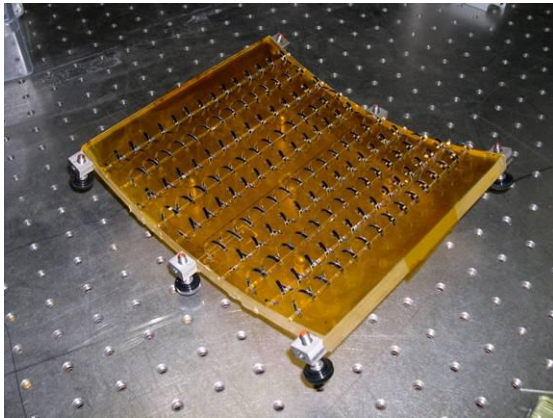
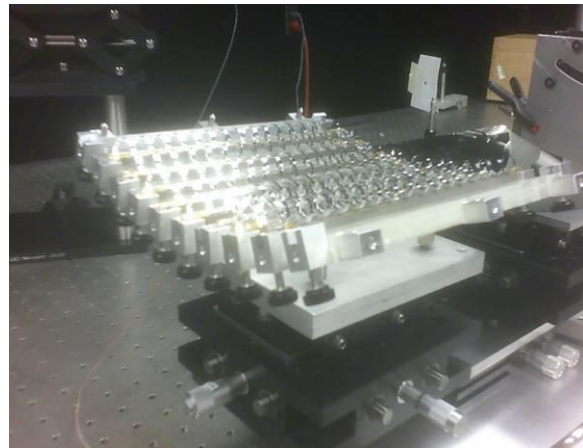


Figure 1: End bonding mount with slumped glass cradle and mylar spring mattress on Kapton base. Three screws at either end serve as the bond points.

Figure 2: Side bonding mount with slumped glass cradle and mylar spring mattress. Height adjustment screws for the mattress springs are visible along the end also visible are brackets for the three side bonds points.



### Alignment testbed

The alignment test-bed (Figure 3) was built to be used as an x-ray-like test as well as for practicing alignment techniques. A Zygo Verifire® interferometer serves as the light source (633 nm) for the test bed and uses a 6" f/3.2 transmission sphere to create a virtual point source. To obtain a collimated beam large enough for our optics, the virtual point source is placed at the focus of a 12 inch diameter off-axis parabola (Due to the large focal length of the optics under test, many fold mirrors are needed to fit the entire test-bed onto one optical bench.) With this as our base setup we are able to view full aperture images of both the primary and secondary focus individually along with the pair focus. Inserting a moveable slit mask before the optics under test, we are also able to perform a grazing -incidence Hartmann test of the surface to better quantify the mirrors focus quality. The 12 inch diameter of the collimated beam also allows us to redirect a portion of the beam not being used by the Hartmann test to a simultaneous normal incidence axial profile measurement. This is particularly useful in monitoring the profiles along the bond points to see how the mirror is affected locally as the bonds cure.

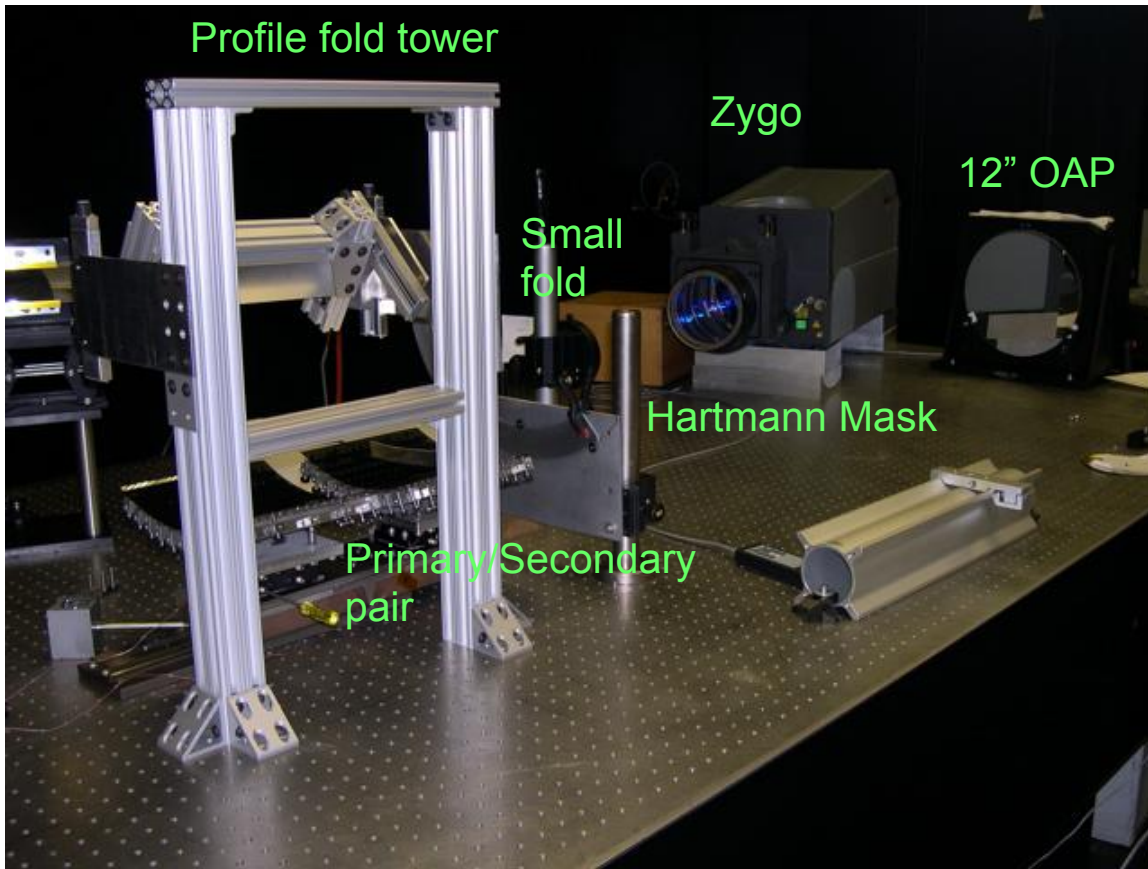


Figure 3: Horizontal Beam Alignment Testbed.

### Alignment

Initial alignment of the mirror in the mattress is critical to the overall alignment procedure. Slight displacements result in noticeable focus irregularities that are difficult to compensate for by adjusting the mattress springs. To accomplish this step fiducials have been placed on the cradle, the kapton mattress base (for the “end bond” system) and the back of each mirror. Careful hand placement is necessary, as the mirror segment tends to settle in a slightly shifted position after the springs have compressed, and the settling is slightly different for each mattress. (see figures 4 & 5). Each cradle has its own 6 degree of freedom (6-DOF) stage. These provide pitch and yaw adjustments to for each mirror segment as well as x and z alignments between the primary secondary pair. The two mirrors are coupled by a third 6-DOF stage which adjusts the Primary/Secondary pair. We are using an Apogee ap47p CCD camera to monitor the focused images. By monitoring the entendu at focus for a primary/secondary pair we are able to use meridonal and transverse adjustments to get registration between the two mirrors. First, however, the individual mirrors have to be dealt with. Typically if anticipating a pair test, the primary mirror is aligned first as its individual characteristics will be masked by the secondary's effects.

The procedure is as follows: first, place the mirror on the mount making sure all fiducials are on top of each other (the mirrors are translucent enough to see all fiducials from above). Good placement, as mentioned previously, is verified by observing the full aperture focused image. Then, again while watching the full aperture image, we determine which mattress springs need to be adjusted to restore the shape of the mirror. During the process, shims on the order of a mm and approximately 50 mm in length are inserted in the full length of the test mirror directly beneath a particular spring row between the mattress and the formed glass cradle. (Figure 1). Shims are no longer needed for this mount and we have finer control on how we affect the mirror shape. Figures 6 & 7 show the before and after shimming full aperture focus images.



Figure 6: Primary focus before shimming

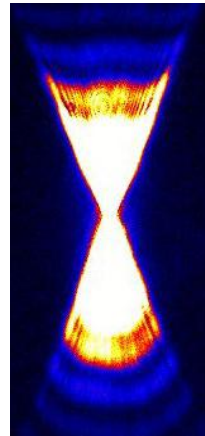


Figure 7: Primary focus after shimming

Note the “S” shape of the diffraction fringes in figure 6 compared to the smooth, rounded fringes in figure 7. This is an iterative process and to a small extent trial and error, Once a good focus image by eye is obtained, however, a 15 or 17 aperture grazing incidence Hartmann test of the surface is taken to verify our improvements.

### **Hartmann Test Results including Sag**

To determine exactly how well the shimming has improved our initial focus, a Hartmann map is generated corresponding to one Hartmann point approximately every 3 degrees. The centroid of each Hartmann position is plotted to form the full map. The Hartmann test probes the first order axial figure vs azimuth – i.e., the local graze angle. But, since the axial figure of a mirror segment is nominally a smooth curve of 1.1 micron P-V, we also need to measure the axial shape vs azimuth in order to build up an accurate geometric model of the mirror segment. We do this by picking off a portion of the collimated beam that is not used in the Hartmann test and use that section for normal incidence interferometry. By reflecting the incident beam off of a rotating fold flat located on the optical axis of mirror segment (the Profile Fold Tower in Figure 3), we can conveniently image a range of azimuthal positions.

Coupling the Hartmann test with the normal incidence axial profiles we can build an accurate wire frame model of each mirror segment, which can be used for ray tracing and prediction of the x-ray imaging performance. Figures 8 & 9 show a typical Hartmann map (with an associated full aperture image) and its corresponding axial profile map. We have also begun fitting our Hartmann data to extract focus and coma errors, as well as fitting the higher order  $\Delta\Delta R$  and out-of-roundness terms, however, these are in the very early stages of development.

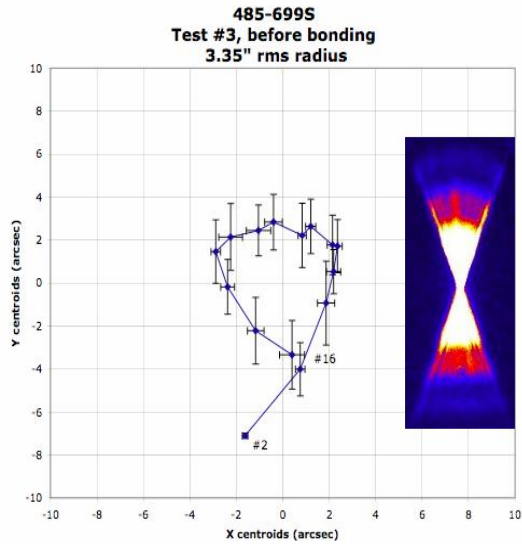


Figure 8: Hartmann map w/ focus image

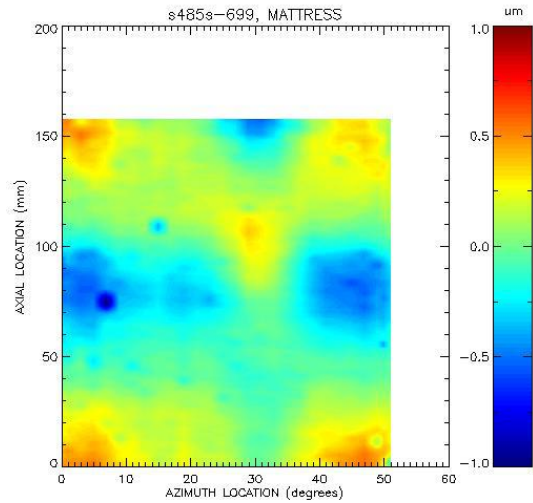


Figure 9: corresponding normal incidence map

## Bonding

The final step in the alignment testing is to tack bond the mirror in place for transport to either the x-ray test facility or into a permanent housing. The bonds need to be strong enough to hold the mirrors final shape after alignment while not distorting the mirror during the bonding process. A bond is deemed successful once both Hartmann and normal incidence maps have shown little change after 1 full week. Initial attempts were made using ADHESIVE A, chosen for its slow cure time (24hrs) and ease in removal. Cured ADHESIVE A is also soft and therefore elastic. The idea is that any temperature (or other environmental) effects will be dampened by the elasticity of the bond. A second bonding material, Adhesive B, was also tested. We can influence the cure rate from 5-45 minutes by varying the catalyst dose. A few different procedures along this line were tested while monitoring the local and global affect on the mirrors. The other relevant variable in this test is the location of the bond points. As discussed earlier there are 3 bond points per end and 5 per side depending on the mount. For the side bonding - two, three and five bond points per side have been explored. For the end bonding - one, two and three bond points per end were investigated.

## Results to date

As stated previously initial testing was performed using the end bond mount and ADHESIVE A. While we were able to align the mirrors to form a good quality focused image (corresponding to a  $\sim 5$  arsec RMS deviation in the Hartmann centroids over a 50 deg segment) the long term stability was not acceptable. As the mirror settled in the mattress over days the static bond points appear as if they bore more of the load and distorted the mirror. The distortions are obvious in the long term focused images (see figure 10 & 11).

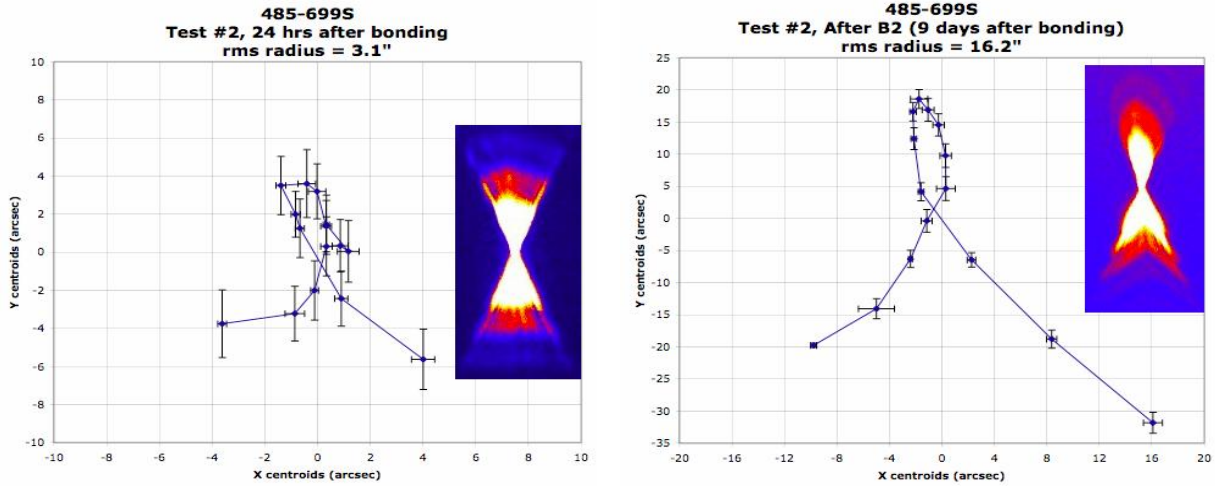
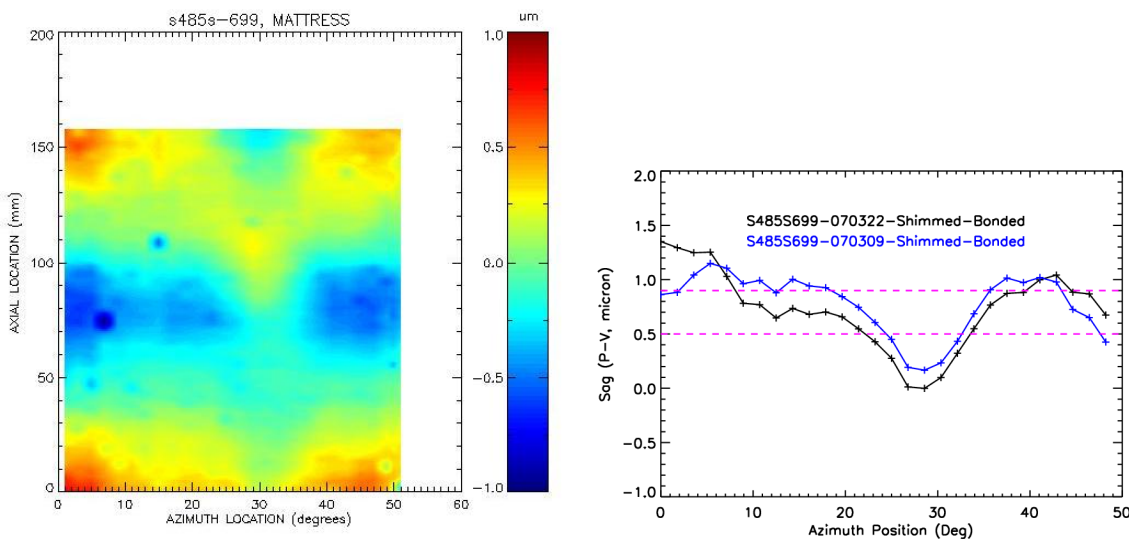


Figure 10 & 11: Focused image and Hartmann maps 24hrs after bonding RMS radius 3.1” and 9 days after bonding RMS radius 16.2”.

The bond pattern for the images in Figs. 10 and 11 was four end bond points just inside the four corners of the mirror. Notice the low flares at the extremes of the image and the high point in the center corresponding to the bond point locations. Adding a third bond at the center complicated this image. Figure 12 shows a focused image after with 3 bonds per end after 10 days

Despite the significant distortions that occurred in the Hartmann map, the axial figure of the mirror segment remains surprisingly stable and consistent from one tack bonding cycle to the next. In Figure 12 the axial figure map corresponding to the Hartmann map in Figure 10 is shown. 13 days later, another set of axial figure was taken, and the axial sag vs azimuth for both sets of data is plotted in Figure 13, demonstrating how stable the axial shape of the mirror is even when significant slope shifts occur.



Figures 12 and 13: Left - the axial figure of the mirror segment corresponding to the Hartmann map shown in Figure 10. Right - the stability of the axial figure is demonstrated by plotting the axial sag vs azimuth for the same mirror segment 13 days apart. Significant changes in the Hartmann map have occurred in that same time, as illustrated in Figure 11.

To further demonstrate the value of the shimming and tack bonding process, the axial figure maps for three separate tack bond cycles using the same mirror segment are shown in Figure 14. The top three plots are the three individual axial figure maps and the bottom three are the difference maps between the first two, the first and last, and the last two maps, respectively. Qualitatively, all three maps are quite similar. Quantitatively, the largest difference is between the first and third maps, which have an RMS difference of 0.105 microns.

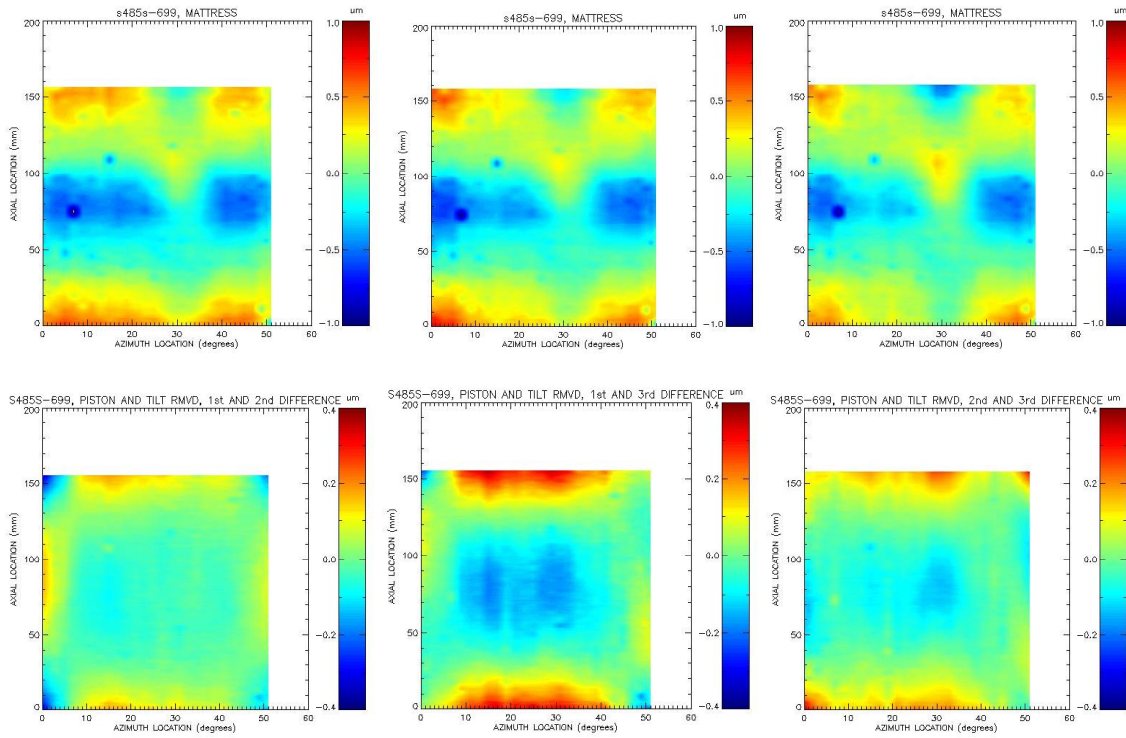


Figure 14. Three sets of axial figure data for three separate tack bond cycles. The top three plots correspond to cycles 1-3, respectively. The bottom three are the difference plots for cycles 1 and 2, cycles 1 and 3, and cycles 2 and 3, respectively.

Another measure of the value of this method for improving focal quality is to plot the axial sag vs azimuth along with that measured without shimming the mattress springs or monitoring the full aperture focus, shown in Figure 15.

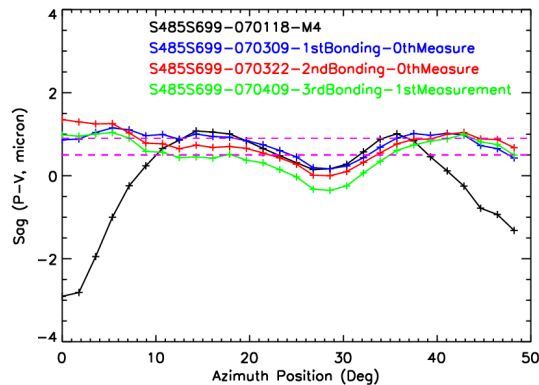


Figure 15. The axial sag vs azimuth for one mirror segment mounted and tack bonded four different times. The black curve corresponds to the axial sag achieved when the mirror segment is simply placed on the mattress without further adjustment of the mattress springs or monitoring the full aperture image. The blue, red and green curves correspond to the 1<sup>st</sup>, 2<sup>nd</sup>, and 3<sup>rd</sup> tack bonding cycles when the full aperture image was monitored while the mattress springs were shimmed to produce an optimal full aperture focus.

Concerned about possible large coefficient of thermal expansion (CTE) mismatch between ADHESIVE A, the steel screw static bond points, and the glass, a new bonding material was chosen. Adhesive B has a more favorable CTE match. The weak ADHESIVE A bond proved to be troublesome when traveling from one testbed to another. If not careful, the bonds would easily break. Adhesive B also cures harder than ADHESIVE A and has a much greater holding power. The focused images, while still exhibiting much the same features as a result of the tack bonding process, improved their long term stability. The axial figures, however, were adversely affected. Side bonding with Adhesive B was attempted both with two and three bond points per side and again the axial figure degradation was deemed acceptable. Conversely, side bonding with ADHESIVE A at two points yielded both excellent long term stability and acceptable axial figure. Table 1 lists significant results. Our efforts have resulted in a method to take a slumped mirror, set it in a temporary mount, and obtain a focused image <5 arcsec RMS and hold this image quality for approximately one week.

**Table 1:** Tack bonding results

Cycle #	Adhesive	# tack points	Before bonding (arcsec rms)	After bonding (arcsec rms)	long term stability
2	ADHESIVE A	4 end points	S - 2.9	S - 3.1	8.6" - 3 days 16.2" - 9 days
3	ADHESIVE A	6 end points	S - 3.35	S - 3.0	3.0" - 4 days 20.9" - 10 days
5	Adhesive B	6 end points	P - 2.3 S - 2.1	P - 1.1 S - 2.3 P/S - 1.5	2.3" - 2 days 3.1" - 8 days 2.3 - 8 days
9	Adhesive B	6 side points	P - 2.8 S - 3.3	P - 5.2 S - 4.4	2.3" - 4 days
13	Adhesive B	4 side points	S- P-1.7	S-9.7 P-4.9 P/S- 6	10.5" - 5 days 8.9" - 5 days
14	ADHESIVE A	4 side points	S- 3.4	S - 2.4	3.6" - 6 days

### Future Directions

In the near future we plan to retest this procedure multiple times to verify our conclusions. We will then be transporting a primary/secondary bonded and aligned pairs to our x-ray testing facility and compare our x-ray results with predictions based on the Hartmann and axial profiling predictions.

In parallel with this effort, we also will be testing the transfer from the temporary mounts discussed here to a permanent housing. This new housing utilizes a side encapsulation method to permanently hold the mirror in the aligned state performed as discussed here.